Copyright © 1973 American Telephone and Telegraph Company
THE BELL SYSTEM TECHNICAL JOURNAL
Vol. 52, No. 2, February, 1973
Printed in U.S.A.

Selectively Faded Nondiversity and Space Diversity Narrowband Microwave Radio Channels

By G. M. BABLER

(Manuscript received August 14, 1972)

The spectral characteristics of nondiversity and space diversity narrowband radio channels subject to multipath fading were estimated from a detailed sampling of channel loss variations as measured on two vertically separated antennas. The data base for this analysis was obtained during a 93-day experiment in which the amplitudes of a set of coherent tones spanning a band of 33.55 MHz and centered at 6034.2 MHz were continuously monitored. The most significant observations were:

(*i*) *For the nondiversity channel, the frequency selectivity of the received transmission loss generally exceeded linear and quadratic components (in frequency) of amplitude distortion for fade depths greater than 30 dB.*

(*ii*) *For the diversity channel constructed by switching between a pair of narrowband channels received on two vertically spaced antennas, the frequency selectivity of the transmission loss was significantly reduced.*

I. INTRODUCTION

During periods of multipath propagation on line-of-sight radio links, deep and selective fading can severely corrupt the desired uniform transmission characteristics of a narrowband microwave channel received on a single antenna. Fortunately, because the multipath processes are sensitive functions of space,[1] the likelihood of simultaneously encountering both deep and frequency-selective fading on two vertically spaced antennas is very small. Earlier studies[2] were directed toward quantification of the spectral and temporal behavior of the amplitude distortion occurring in a nondiversity narrowband radio channel derived from a single receiving antenna. In the present paper, we describe a second experiment undertaken in 1971 to extend the

nondiversity measurements and to examine the amplitude distortions occurring in a diversity channel derived from the narrowband signals received on a pair of vertically spaced antennas.

The data used in this analysis were taken between June 16 and September 16, 1971 (93 days), and included the amplitude measurement of 62 uniformly spaced, coherent tones spanning 33.55 MHz at 6 GHz transmitted over a 26.4-mile radio path and received on two antennas of vertical separation of 19 feet 3 inches. The tone fields received on the two antennas were sampled five times per second and the results recorded whenever significant amplitude activity was occurring anywhere in either channel.

The paper is organized in the following order: (*i*) description of the experiment, (*ii*) a discussion of the occurrence of fading throughout the 1971 fading season, and an identification of the data base for analysis, (*iii*) characterizations of the nondiversity, and (*iv*) diversity amplitude distortions.

II. SUMMARY

A condensed listing of the findings follows:

(*i*) The fade depth distributions for individual tones had the expected slopes[3] of a decade of probability of occurrence per 10 dB change in fade depth with the lower antenna undergoing somewhat less fading.

(*ii*) The statistical distributions of linear and quadratic amplitude distortion of the nondiversity channel exhibited slopes of a decade of probability per 10 dB change in distortion. For a narrow channel bandwidth of 19.8 MHz, the linear and quadratic distortion exceeded 18.5 and 7 dB, respectively, for 10^{-5} of the observation time.

(*iii*) For the nondiversity channel, the amplitude distortion generally exceeded second order for fade depths greater than 30 dB and contained higher-order components in frequency selectivity.

(*iv*) The statistical distributions of linear and quadratic amplitude distortion of the diversity channels derived by threshold or comparative switching exhibited slopes of a decade of probability of occurrence per 5 dB change in distortion. For a bandwidth of 19.8 MHz, and for 10^{-5} of the time, a -30-dB threshold diversity channel experienced linear and quadratic distortions exceeding 10 and 2.8 dB, respectively, and a comparative diversity channel experienced distortions of 8.6 and 2.2 dB, respectively.

(*v*) For the diversity channels, the amplitude distortion generally exceeded zeroth-order for fade depths greater than 10 dB.

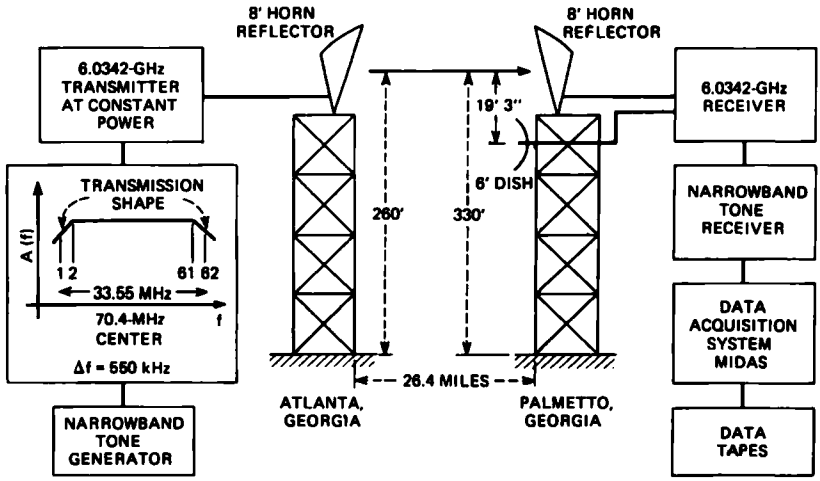

Fig. 1—Experimental arrangement on the Atlanta to Palmetto, Georgia, radio link.

III. EXPERIMENTAL DESCRIPTION

3.1 *The Experiment*

The 1971 measuring arrangement shown in Fig. 1 was essentially the same as the previous year which has been described elsewhere.[2] To review briefly, a flat and constant in time narrowband field of 62 coherent tones spaced 550 kHz apart and centered at a radio frequency of 6.0342 GHz was radiated from a standard horn reflector antenna at a microwave radio relay tower outside of Atlanta, Georgia. The signal, after propagating 26.4 miles along a line-of-sight path, was

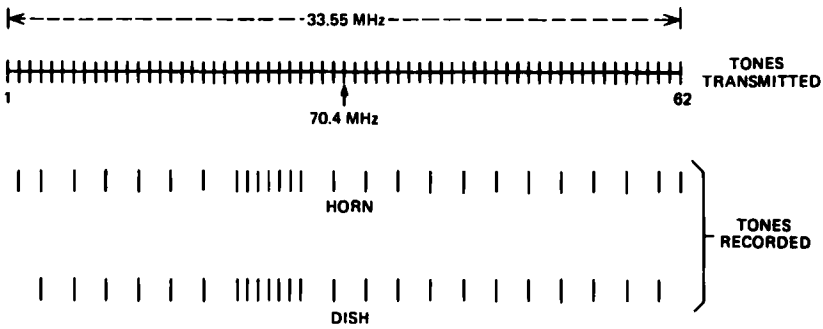

Fig. 2—Subset of tones transmitted and recorded serially on the horn reflector and dish antennas at Palmetto.

intercepted by two antennas: a standard horn reflector with a 1.25-degree half-power beamwidth and a 6-foot dish with a 2-degree half-power beamwidth separated 19 feet 3 inches apart and mounted on a microwave tower at Palmetto, Georgia. Both images of the narrowband tone fields were translated to an intermediate frequency where a tone receiver selected tones for a power measurement. The subset of transmitted tones measured and recorded are shown in Fig. 2; the amplitude quantization was 1 dB, the time quantization was 0.2 second. A multiple input data acquisition system (MIDAS) supervised the measurement and recording of amplitude levels and time as well as controlled the recording rates according to the tone activity.

The reference levels for both tone fields were determined by statistical studies of tone amplitudes during midday, nonfading periods. The rms variation in the reference levels was less than the amplitude quantization size of 1 dB.

IV. OCCURRENCE OF FADING ACTIVITY

The fading activity of the tone fields received on both antennas was continuously monitored from June 16 to September 16, 1971, and recorded for almost all of the 93 days (8.0352×10^6 seconds). The recorded data base, written by MIDAS and stored on 34 magnetic tapes, was condensed to include all periods with any fading in excess of 10 dB with respect to midday normal. This process compressed the time span of the data base to 1.28×10^6 seconds.

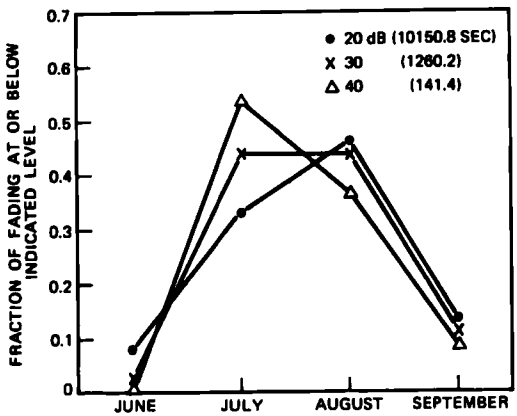

Fig. 3—Occurrence of fading for midchannel tone 24 received on the horn reflector antenna throughout the 1971 measurement period.

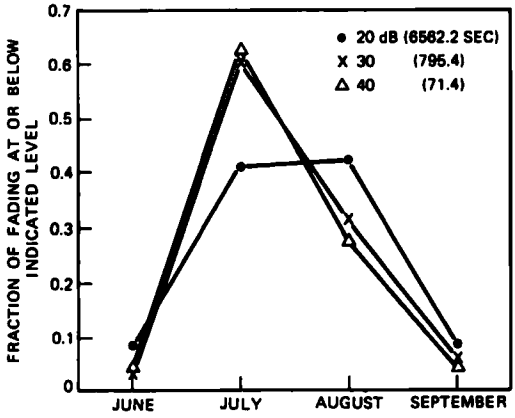

Fig. 4—Occurrence of fading for midchannel tone 24 received on the dish antenna throughout the 1971 measurement period.

The data for a selected set of tones in both narrowband channels was processed to determine the total time during which any tone was faded below signal levels. An overview of the fading activity measured

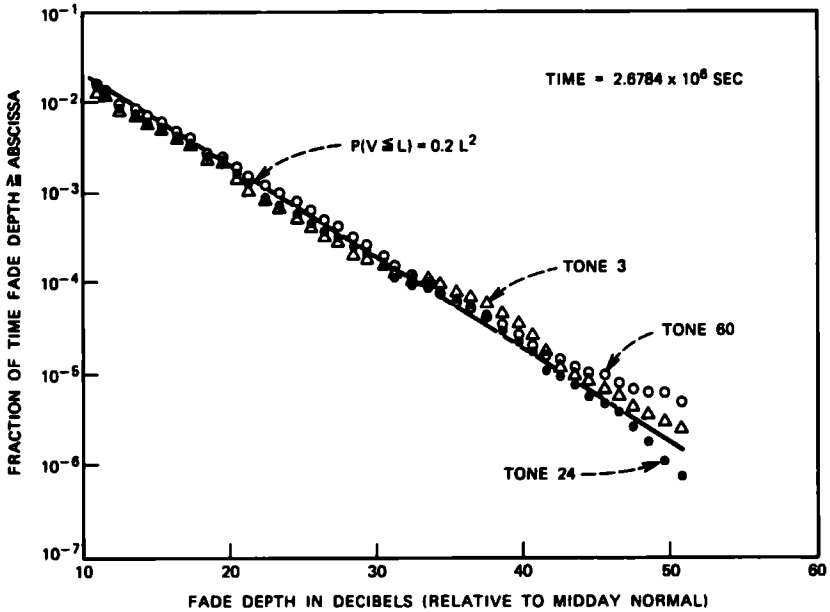

Fig. 5—Fade depth distributions for tones 3, 24, and 60 received on the horn reflector antenna for the month of August.

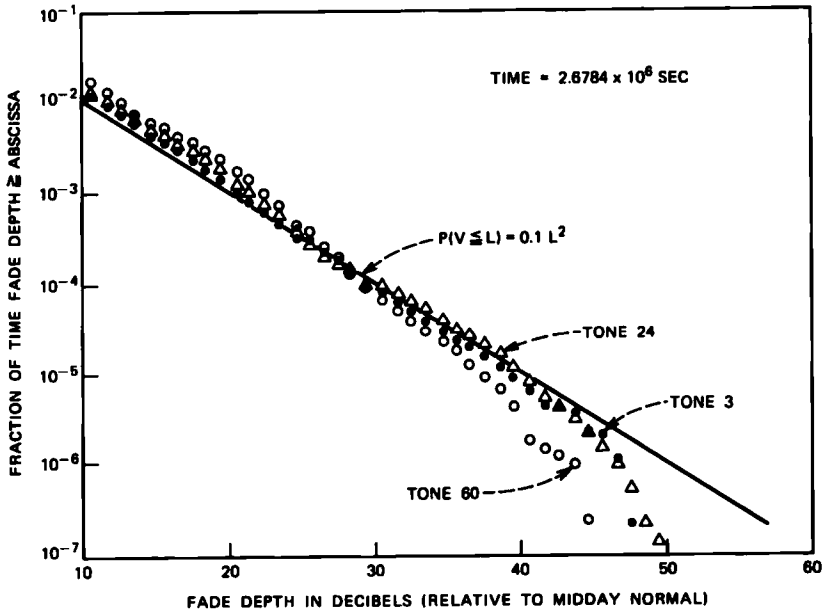

Fig. 6—Fade depth distributions for tones 3, 24, and 60 received on the dish antenna for the month of August.

during the fading season in Georgia and lumped into month categories of a single midchannel tone, tone 24, received on the horn and dish antennas is shown in Figs. 3 and 4, respectively. The occurrence of midchannel fading for both antennas is far less in the June and September periods than for July or August. In addition, we observed more midchannel fading for both antennas at and below 30 dB in July than in August, but the relative occurrence of fading at the 20, 30, and 40 dB levels and intermediate levels was more evenly balanced in August than in July. Because we desire to have a set of fading samples uniformly spread across all fade depths with no particular levels dominating the transmission loss statistics on either antenna, the month of August was selected as the working data base to be used in the characterization of the frequency-selective fading occurring in both channels.

The fade depth distributions for tones 3, 24, and 60 received on the horn and dish antennas are given in Figs. 5 and 6, respectively. The ordinate is the fraction of 2.6784×10^6 seconds (number of seconds in August) that the tones were faded the amount indicated on the

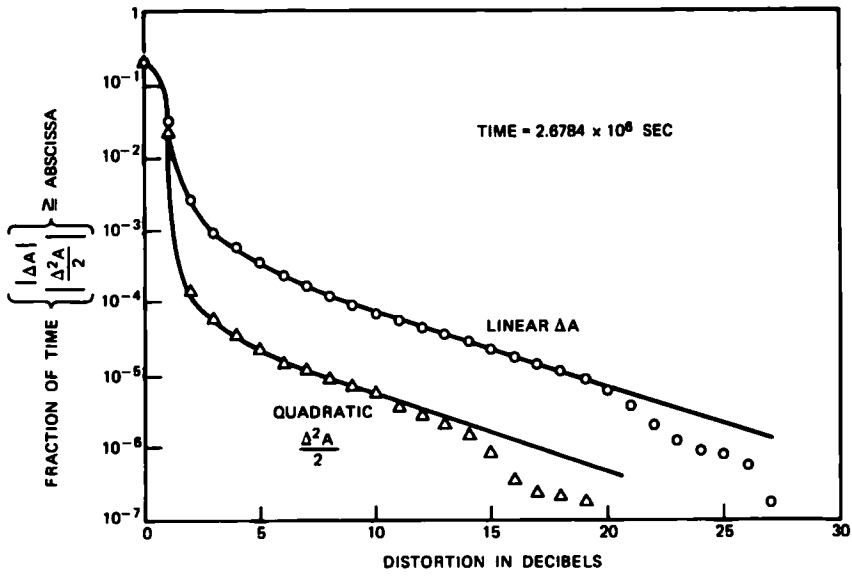

Fig. 7—Unconditional linear and quadratic distortion distributions for the 19.8-MHz nondiversity (horn reflector antenna) channel.

abscissa. The amplitudes, V, of the tones received on both antennas faded below signal levels, L, according to the expected fade depth distribution relation[3]

$$P(V \leqq L) = aL^2 \quad \text{for} \quad L \leqq 0.1 \ (20 \text{ dB}) \tag{1}$$

where fade depth $A = -20 \log L$ and where, for the August period, the proportionality constants a (functions of the radio paths' electromagnetic environment) were found to be $a = 0.2$ for the horn antenna and $a = 0.1$ for the dish antenna. The fact that, throughout the month, the lower dish antenna experienced less fading than the horn antenna reflects the spatial sensitivity of the fading processes and not the small differences in antenna beamwidths. Calculations based on an empirical formulation of the occurrence of multipath fading[4] indicate for the Atlanta-Palmetto 26.4-mile path at 6 GHz, $a \cong 0.27$. The conclusion is that, whereas the fading activity observed on both antennas was somewhat less than expected, the data base for the horn antenna is improved over the previous year.[2]

A second and important observation is that the fade depth distributions of all three tones on both antennas are essentially the same, indicating a nonpreferential amount of fading in the channels which

was not the case in the samples of the 1970 study. This more uniform set of fade samples across the narrowband channels, as well as the somewhat greater number of events, result in an improved understanding of frequency-selective fading in single and pairs of narrowband radio channels.

V. THE NONDIVERSITY CHANNEL SELECTIVITY CHARACTERIZATION

The degree of frequency selectivity which occurred in the nondiversity channel was characterized by statistical distributions of linear $(\Delta A = A(f_3) - A(f_1))$ and quadratic $(\Delta^2 A/2 = (A(f_1) + A(f_3))/2 - A(f_2))$ amplitude distortion constructed from three uniformly spaced samples of transmission loss in dB $(A(f_1), A(f_2), A(f_3))$. The distributions for the linear and quadratic distortions occurring across a 19.8-MHz nondiversity channel (the signal from the horn antenna) are shown in Fig. 7. The abscissa is the amount of distortion in dB, and the ordinate is the fraction of 2.6784×10^6 seconds (August). The distributions exhibit slopes of a decade of probability of occurrence per 10 dB change in distortion with the linear distortion $\Delta A \geqq 18.5$ dB and the quadratic distortion $\Delta^2 A/2 \geqq 7$ dB for 10^{-5} of the time (about 27 seconds). The roll-off of the curves below 10^{-5} is a too-few-samples effect. For high-performance microwave radio systems the smallest

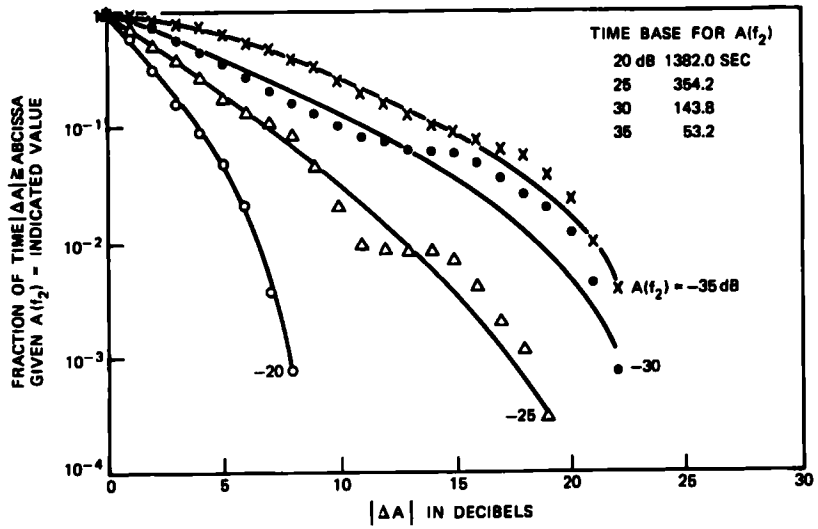

Fig. 8—Conditional linear distortion distributions for the 19.8-MHz nondiversity channel.

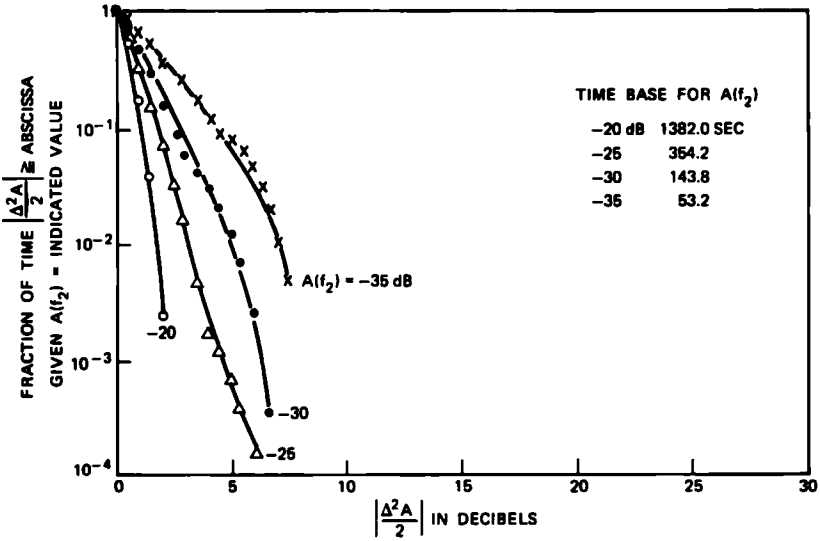

Fig. 9—Conditional quadratic distortion distributions for the 19.8-MHz nondiversity channel.

fraction of time for single-link consideration is approximately 10^{-5}, or a few tens of seconds per month. For larger fractions of time the data show excellent point-to-point consistency.

The linear and quadratic distortion distributions conditioned on fade depth of the midchannel tone $[A(f_2)]$ are shown in Figs. 8 and 9, respectively. The time base for each curve is indicated by the fade depth. Although the distortion curves have some point scatter, the curve-to-curve placement is improved over the 1970 sample.[2] In addition, we note that at each fade depth the channel experienced more linear and less quadratic distortion in 1971 as compared to the 1970 sample. Because there were more deep fading events in 1971 than 1970, and because there was more linear distortion at each fade depth in 1971 than 1970, we can conclude, as shown in Fig. 7 of this paper and Fig. 12 of Ref. 2, that there was more linear distortion in the channel. No similar arguments can be made for the quadratic distortion because of conflicting occurrences of distortion and fade depth for both years, although we do note that the 1971 channel suffered less quadratic distortion. The rate of growth of the linear and quadratic distortion which occurred in the nondiversity channel with increasing bandwidth and fade depth was essentially the same as the 1970 data (and is shown in Fig. 16).

Higher-order selective effects were again studied by accumulating the distributions of the maximum amplitude difference, called MAX|ERROR|, between the observed channel loss samples $A^M(f)$ and a three-term power series quadratic approximation constructed from the linear and quadratic distortion parameters. Thus

$$\text{MAX|ERROR|} = \text{MAX}\left|\left\{\underbrace{A^M(f)}_{\substack{\text{Measured Samples}\\ \text{of Channel Loss}}} - \underbrace{\left[A(f_2) + \frac{\Delta A}{2}\left(\frac{f-f_2}{\Delta f}\right) + \frac{\Delta^2 A}{2}\left(\frac{f-f_2}{\Delta f}\right)^2\right]}_{\text{Quadratic Power Series Approximation}}\right\}\right|.$$

Fig. 10 shows the occurrence of MAX|ERROR| events for all fade depths (an unconditional distribution) and Fig. 11 shows the conditional distributions of MAX|ERROR| events for individual fade depths. The unconditional distribution of MAX|ERROR| for a bandwidth of 19.8 MHz is approximately the same as the 1970 data for a bandwidth of 20.35 MHz. The conditional distributions indicate

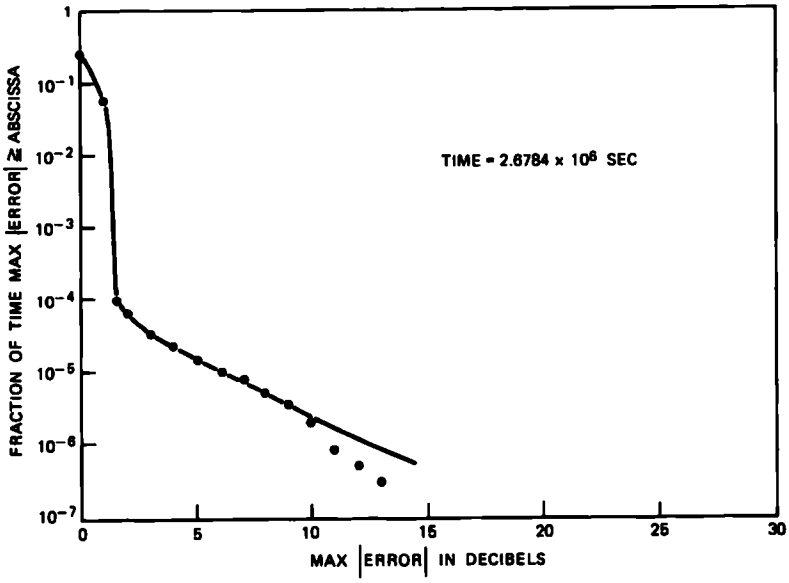

Fig. 10—Unconditional distribution of the MAX|ERROR| for the 19.8-MHz nondiversity channel.

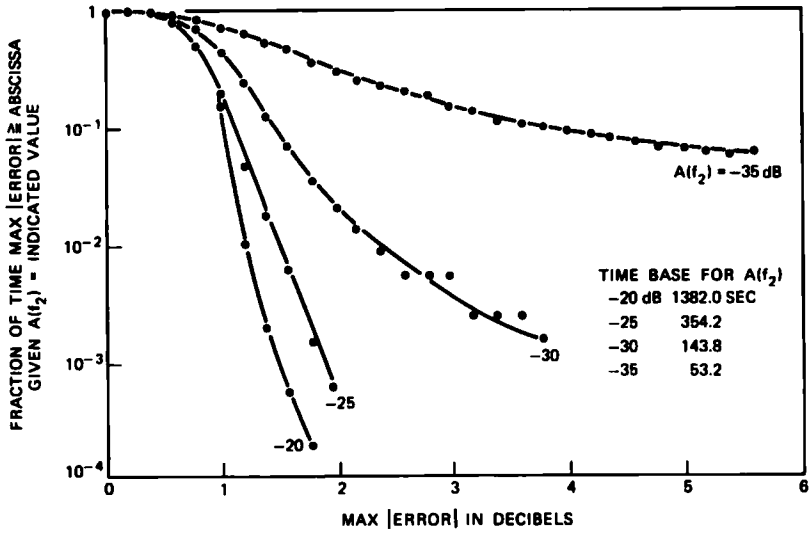

Fig. 11—Conditional distributions of MAX|ERROR| for the 19.8-MHz nondiversity channel.

rapid growth in the difference between the three-term power series approximation and the actual channel loss at and below the 30-dB fade level. For fade depths greater than 30 dB, the observed amplitude-frequency selectivity structure of the nondiversity narrowband radio channel's transmission loss exceeded linear and quadratic components (in frequency) of amplitude distortion by 2 dB as was observed previously in the 1970 narrowband data.

VI. THE DIVERSITY CHANNEL SELECTIVITY CHARACTERIZATION

One form of protection against deep and selective fading in a narrowband radio channel during periods of multipath propagation is to derive a diversity channel from the narrowband signals received on a pair of vertically spaced antennas. For the deeper fades, the reduction in number and duration of fading events increases significantly, since deep fades rarely occur simultaneously on two vertically spaced antennas.[1] Because amplitude distortion (linear, quadratic, and higher orders of structure) is present for only the deeper fades, the likelihood of simultaneously encountering deep fading with large degrees of amplitude distortion on two antennas is indeed rare.

To demonstrate the variety and nature of the measured transmission loss as simultaneously observed in the space diversity pair of narrow-

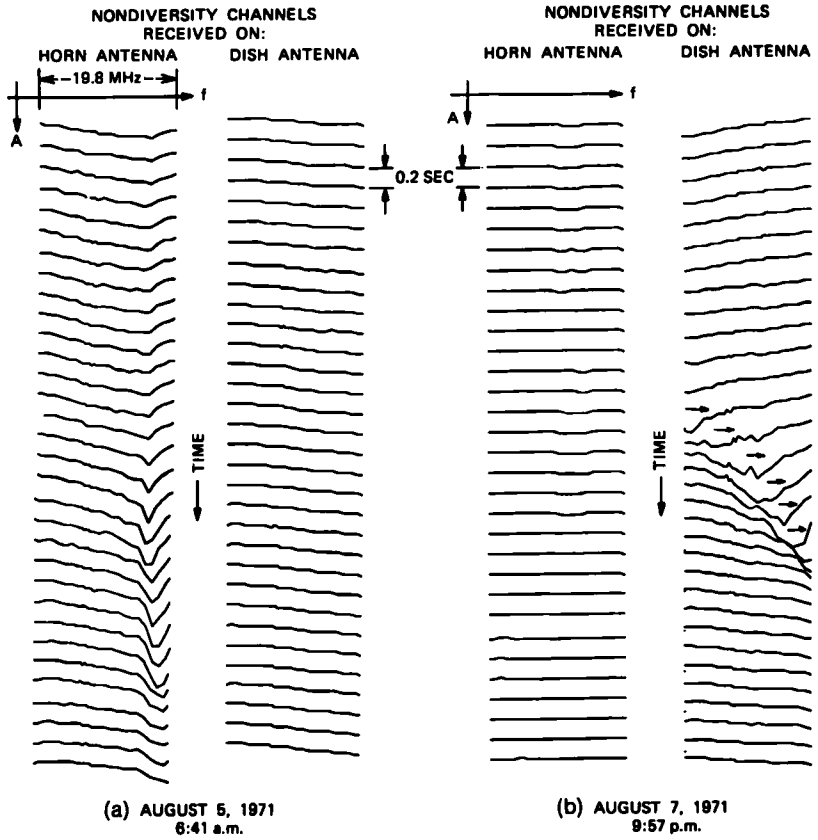

Fig. 12—Time sequential plots of the measured transmission losses simultaneously occurring in the narrowband channels received on the horn reflector and dish antennas.

band channels during the 1971 period, and to motivate the diversity channel construction algorithms, two fading periods are presented in Figs. 12a and 12b. Displayed is the simultaneous time sequential state of the channel transmission loss of the tone fields as measured on the horn and dish antennas. An arbitrary 0-dB transmission loss reference has been employed for figure compactness; the time between scans was 0.2 second.

In event (a), the selectivity develops at the upper edge of the narrowband channel received on the horn antenna and then moves out of channel. The narrowband channel as received on the dish antenna was simultaneously undergoing about 5 dB of linear distortion super-

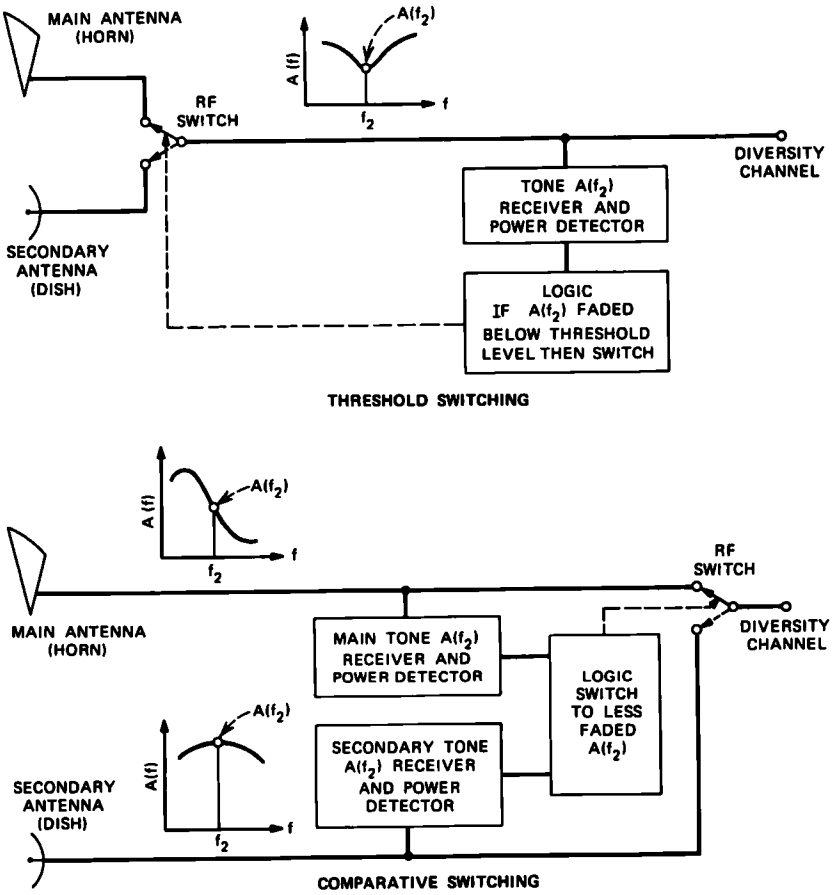

Fig. 13—Diversity channel construction schemes.

imposed on a broader-band nonselective fade. In event (b), the horn antenna suffers only slight nonselective transmission loss, while the dish antenna experiences a rapidly moving selective fade. Most of the fading events observed were similar to events (a) or (b); generally, when there was deep fading with appreciable amplitude distortion in one channel, the alternate channel was undergoing only shallow fading.

In Section 6.1 we describe how narrowband diversity channels were constructed from the space-diversity measurements of the 1971 period and the characterization of the observed diversity narrowband channel amplitude distortions.

6.1 *The Diversity Channel Construction*

The objective of diversity construction is to derive a new narrowband channel undergoing less fading and consequently less amplitude distortion. Two straightforward idealized switching algorithms (schemes), threshold switching and comparative switching, have been examined and are presented schematically in Fig. 13.

In threshold switching, a single narrowband threshold detector measures the power at the center of the narrowband tone field [say at $A(f_2)$] received on the presently connected antenna, and only if

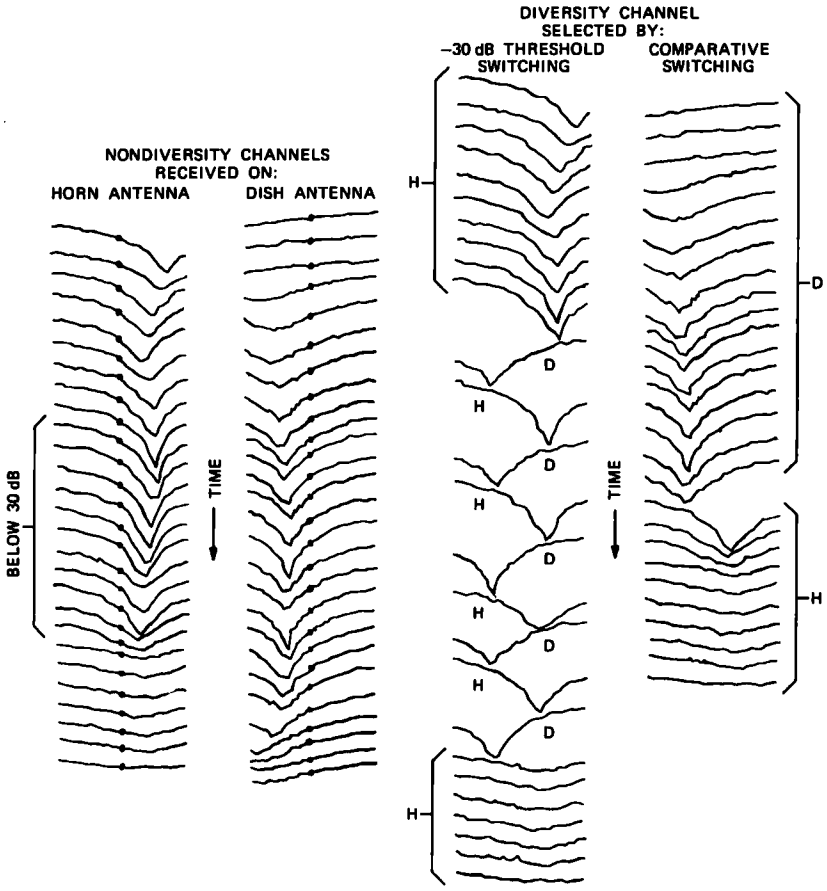

Fig. 14—Time sequential plots of the nondiversity and diversity channel transmission losses.

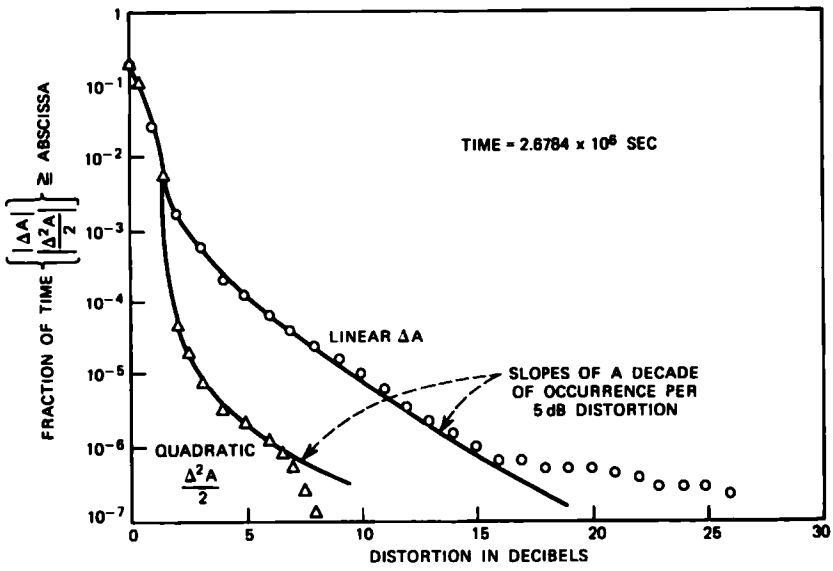

Fig. 15—Unconditional linear and quadratic distortion for the 19.8-MHz, −30-dB threshold diversity channel.

this power falls below some fixed threshold level, system logic directs a radio frequency (RF) switch to select the alternate antenna. If the midchannel power on the secondary antenna is (or falls) below the threshold level, the main antenna is reconnected. The second switching scheme studied, comparative switching, employs two separate receivers which simultaneously monitor the midchannel power of the narrow bands received on both antennas and direct the RF switch to connect in the antenna with greater midchannel power. Both forms of channel construction, threshold and comparative switching, result in a newly derived diversity channel undergoing less fading and consequently less amplitude distortion.

For the selective events displayed in Fig. 12, both switching schemes would result in the selection of the less selectively faded antenna. The resulting diversity channel would therefore be the dish in event (a) and the horn in event (b). To serve as an additional instructive example, in Fig. 14 is shown the channel activity of a diversity channel constructed from the nondiversity channels which are simultaneously undergoing selective fading. The threshold diversity channel is the result of 10 switches between antennas beginning and ending the displayed period on the horn antenna. Because both antennas' mid-

channel power levels are below the −30-dB threshold level, the cycle time between nondiversity channels is 0.2 second. For this particular set of events, contrary to those of Fig. 12, the threshold diversity channel's amplitude distortion is not significantly improved over either nondiversity channel because of the simultaneously occurring selective fading in both antennas. The comparative diversity channel, the result of a single switch between antennas, experiences less amplitude distortion than either nondiversity channel. The events as indicated in Fig. 12 are much more frequent than the highly selective and rare events as displayed in Fig. 14.

By using the real-time measurements of transmission loss simultaneously occurring in both narrowband channels and computer programs to simulate the switching schemes, the linear and quadratic amplitude distortion distributions for the diversity channels were accumulated both for unconditional and conditional fade depths [conditioned on the diversity channel's tone, $A(f_2)$] as well as for different bandwidths. These results follow.

6.2 *The Threshold Diversity Narrowband Channel*

The unconditional linear and quadratic distortion distributions for the 19.8-MHz-wide threshold diversity channel are shown in Fig. 15. A threshold level of −30 dB was chosen because it is at and below this level that the amplitude distortion of a nondiversity channel exceeds second-order selectivity and it is these higher-order distortion events we wish to avoid by the antenna selecting process. For a band-

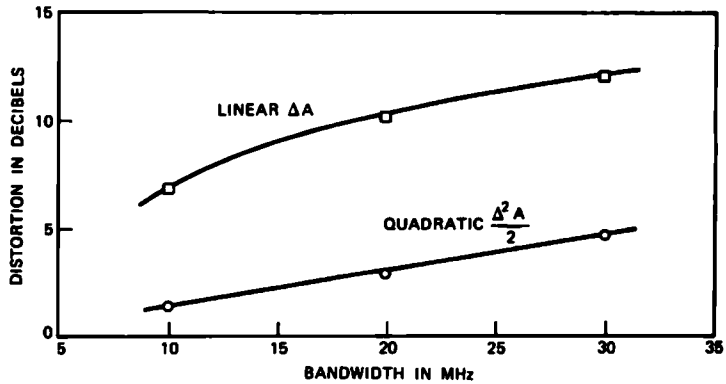

Fig. 16—Growth of linear and quadratic distortion with bandwidth for the nondiversity channel and the −30-dB threshold diversity channel for a fixed 10^{-3} fraction of the time.

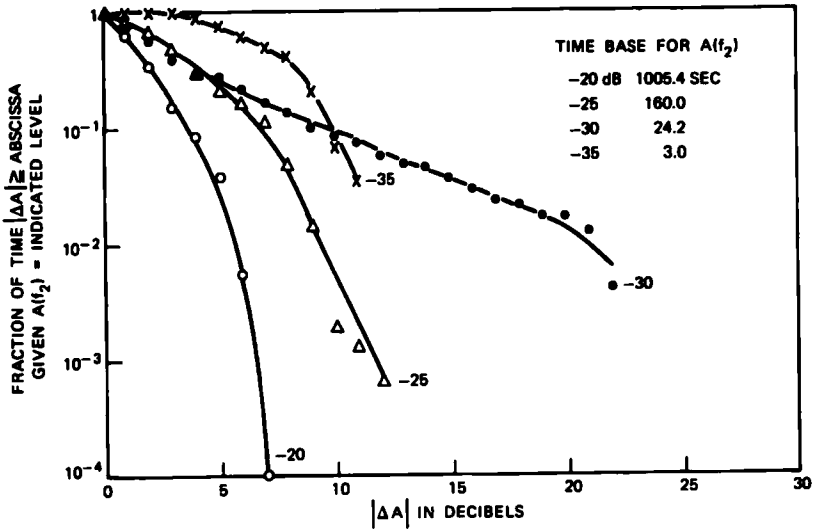

Fig. 17—Conditional linear distortion distributions for the 19.8-MHz, −30-dB threshold diversity channel.

width of 19.8 MHz, the linear and quadratic distortions exceeded 10 and 2.8 dB, respectively, for 10^{-5} of the time. Contrasting Figs. 7 and 15, we find for 10^{-5} fraction of the time that the −30-dB threshold switching procedure has reduced the linear and quadratic amplitude distortions by 46 and 60 percent, respectively, over the distortions occurring in the nondiversity channel. The distributions of distortion for the −30-dB threshold channel exhibit slopes of a decade of probability of occurrence per 5 dB change in distortion. Although the data points below 10^{-6} are less reliable because of fewer samples, the roll-up at the tail of the linear distortion distribution is real and represents a few events spanning a few seconds during the 2.6784×10^6 seconds of measurement where severe fading below 30 dB was simultaneously occurring in both narrowband radio channels. The distributions for other bandwidths of the threshold channel were similar in shape to those presented in Fig. 15; the rate of growth in distortion with bandwidth, as indicated in Fig. 16, was about half the nondiversity channel's rate. The −30-dB threshold diversity channel was the result of 103 switches between antennas.

The conditional distributions of distortion are shown in Figs. 17 and 18. The distributions show the expected reduction in linear distortion as compared to the nondiversity channel, Fig. 8, for fades not exceeding

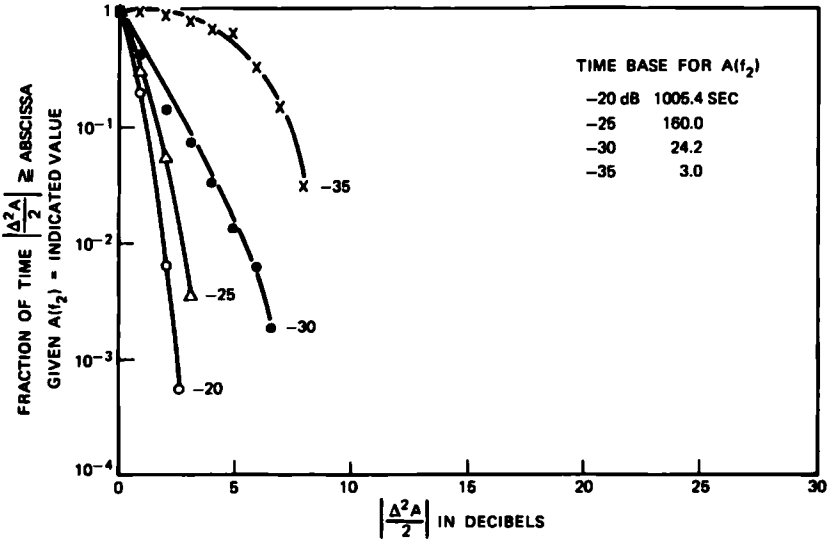

Fig. 18—Conditional quadratic distortion distributions for the 19.8-MHz, −30-dB threshold diversity channel.

30 dB. The roll-up of the distribution for 30-dB fades is the result of two effects: depletion of shallow structure (small linear distortion) events due to the threshold switching action and the over-abundance of a few high structure events at the 30-dB level. The roll-off of the 35-dB fade distribution is the result of too few samples. The distributions of the observed quadratic distortion at the various fade depths, Fig. 18, show a more uniform curve-to-curve behavior and indicate approximately the same amounts of distortion at each fade depth as the nondiversity channel. The 35-dB fade depth curve again has insufficient samples.

These results show that a diversity channel selected according to the −30-dB threshold scheme outlined above undergoes significantly less overall amplitude distortion and presents to the radio sytem a more uniform and desirable transmission loss characteristic. Higher-order structure of the threshold diversity channel will be discussed in Section 6.4

6.3 *The Comparative Diversity Narrowband Channel*

The unconditional linear and quadratic distortion distributions for the 19.8-MHz-wide comparative diversity channel are shown in Fig. 19. Contrasting Figs. 15 and 19, we observe that the comparative di-

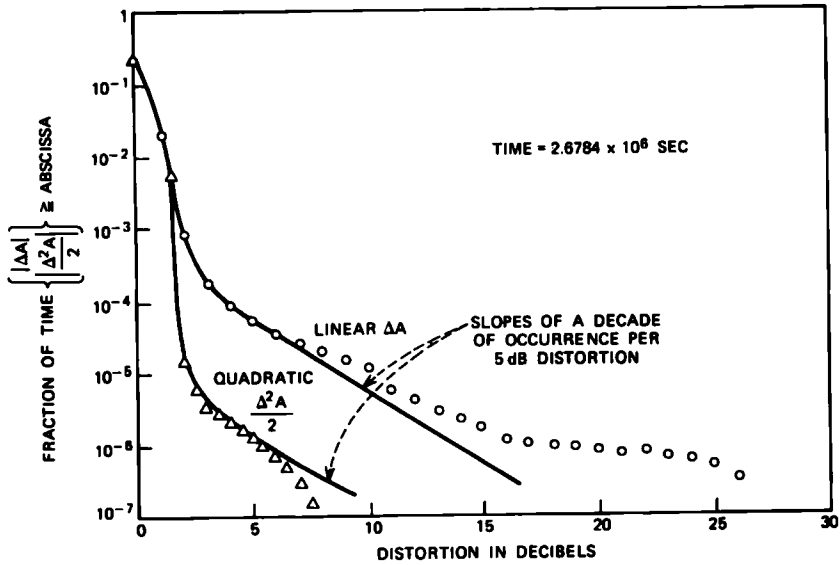

Fig. 19—Unconditional linear and quadratic distortion distributions for the 19.8-MHz comparative diversity channel.

versity channel experienced less linear and quadratic distortion than the threshold diversity channel. For a bandwidth of 19.8 MHz, the linear and quadratic distortions of the comparative diversity channel exceeded 8.7 and 2.2 dB, respectively, for 10^{-5} of the time. Again we note that the distributions for the diversity channel exhibit slopes

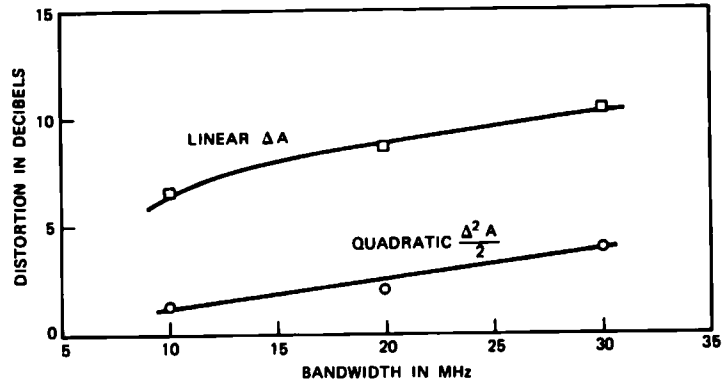

Fig. 20—Growth of linear and quadratic distortion with bandwidth for the comparative diversity channel for 10^{-5} of the time.

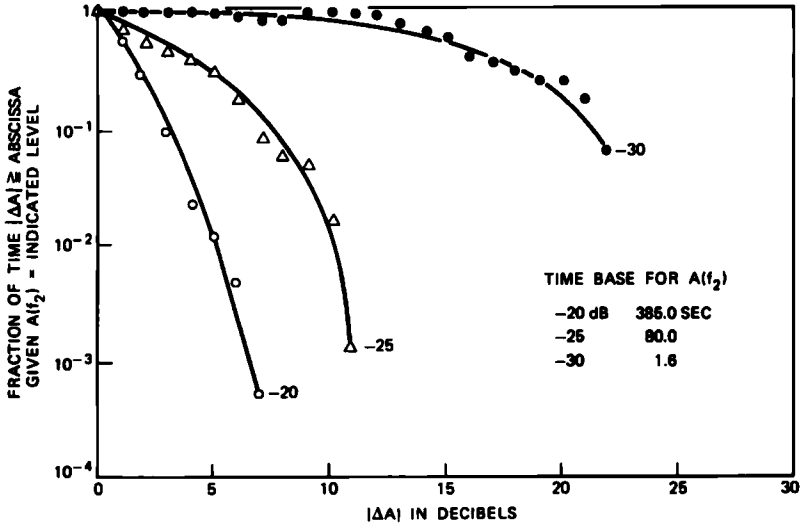

Fig. 21—Conditional linear distortion distributions for the 19.8-MHz comparative diversity channel.

of a decade of probability of occurrence per 5 dB change in distortion. The scatter and roll-up at the tail for the linear distribution represents several seconds of fading events at which time both channels were undergoing significant linear amplitude distortion. The distributions for other bandwidths of the comparative diversity channel were similar

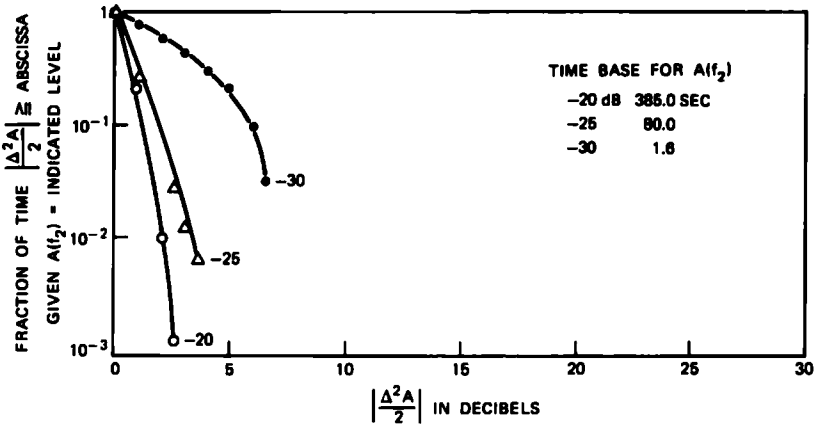

Fig. 22—Conditional quadratic distortion distributions for the 19.8-MHz comparative diversity channel.

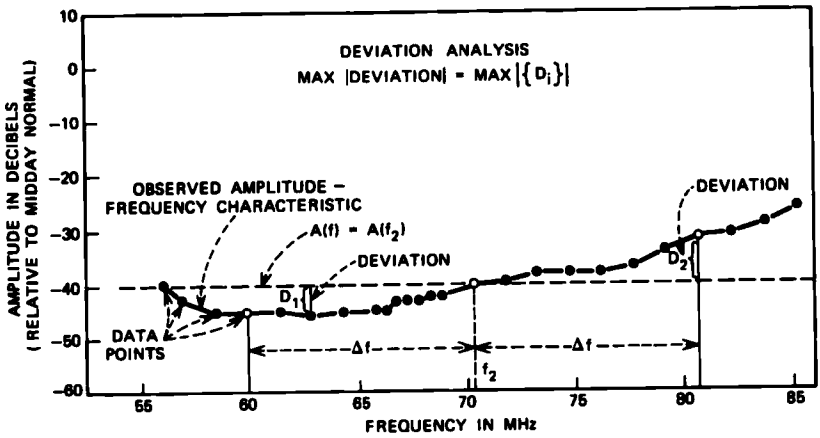

Fig. 23—Definition of deviations between the observed channel loss (solid line) and the zeroth degree, midchannel level approximation (dashed line).

in shape to those presented in Fig. 19 and again the rate of growth in distortion with bandwidth was about half the nondiversity channel's rate as indicated in Fig. 20. The comparative diversity channel was the result of 5873 switches between antennas.

The conditional distributions of distortion are shown in Figs. 21 and 22 and show approximately the same amounts of amplitude distortion as the nondiversity channel for fade depths not exceeding 30 dB. The distributions for the 30-dB level have been included for completeness but are less reliable because of too few samples.

6.4 *Error Analysis of the Higher-Order Distortion*

As previously discussed in Section V, the selectivity structure within a narrowband channel increases with fade depth, and for the nondiversity channel, the selectivity structure exceeds second order for fades in excess of about 30 dB. For the diversity channels constructed by threshold and comparative switching, we found that those fading events with large linear and quadratic amplitude distortion were significantly reduced. Clearly, if a nondiversity channel does not exceed second order for fades not in excess of 30 dB, a diversity channel not undergoing fades in excess of 30 dB will also not exceed second order. Thus, rather than compute and construct the statistical distributions for the maximum amplitude difference between the observed channel loss and a three-term power series quadratic approximation as we did for the nondiversity study, we choose to redefine the errors as

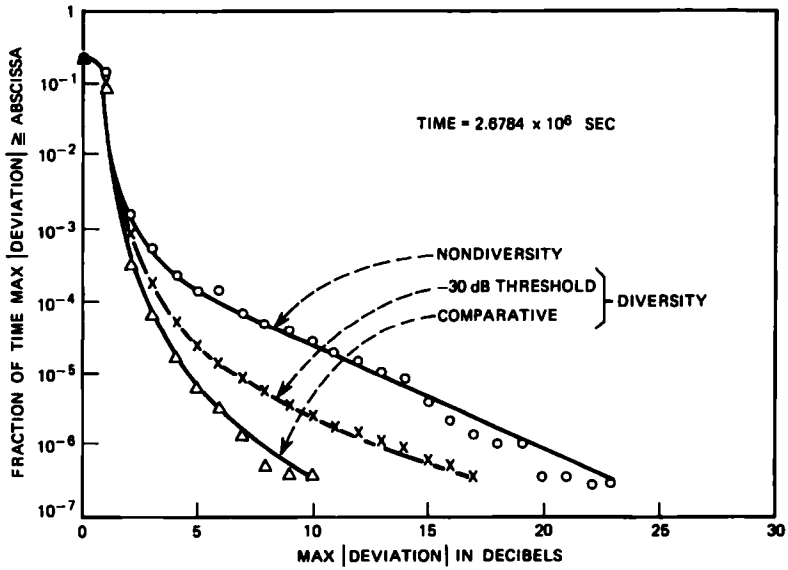

Fig. 24—Unconditional distributions of MAX|DEVIATION| for the nondiversity and diversity channels of bandwidth of 19.8 MHz.

the deviations, D, between the measured samples of transmission loss, $A^M(f_i)$, and a one-term power series approximation constructed from the midchannel loss $A(f_2)$. That is,

$$D_i = D(f_i) = \underbrace{A^M(f_i)}_{\substack{\text{Measured Samples of Transmission Loss}}} - \underbrace{A(f_2).}_{\substack{\text{Midchannel Loss}}} \tag{2}$$

Figure 23 shows the observed selectivity, the zeroth-degree, midchannel level approximation, and two of the deviations. The maximum of the inband amplitude deviation, called MAX|DEVIATION|, was monitored for both forms of diversity channels and is now presented in Fig. 24. For completeness and for comparison, the nondiversity channel's MAX|DEVIATION| distribution is included. Both forms of diversity channels show significant reduction in maximum deviation as compared to the deviation experienced by the nondiversity channel. The marked reduction in deviations for the diversity channels was a result of less deep fading events in the diversity channels.

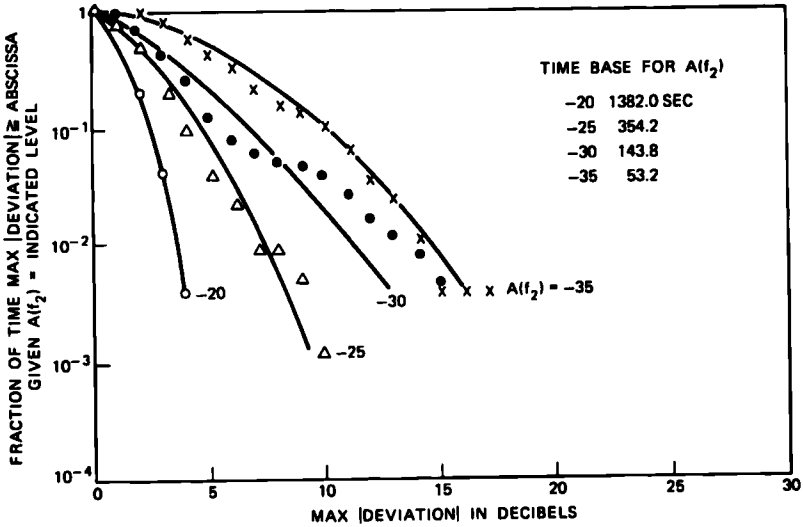

Fig. 25—Conditional distributions of MAX|DEVIATION| for the 19.8-MHz nondiversity channel.

The amplitude deviation distributions conditioned on the mid-channel fade depth for the diversity channels were similar to those for the nondiversity channel which are presented in Fig. 25. For fade depths greater than 10 dB, the observed amplitude selectivity structure of the diversity (and nondiversity) narrowband channels exceeded zeroth order by 2 dB. This is in agreement with the observation that both forms of diversity switching may significantly protect the radio channel from deep selective fading events but not from the less faded channels which experience linear amplitude distortion.

VII. ACKNOWLEDGMENTS

Indebtedness for the experimental data is extended to my colleagues W. T. Barnett, G. A. Zimmerman, and C. H. Menzel. The interest and support of E. E. Muller were invaluable.

REFERENCES

1. Vigants, A., "The Number of Fades in Space-Diversity Reception," B.S.T.J., *49*, No. 7 (September 1970), pp. 1513–1530.
2. Babler, G. M., "A Study of Frequency Selective Fading for a Microwave Line-of-Sight Narrowband Radio Channel," B.S.T.J., *51*, No. 3 (March 1972), pp. 731–757.
3. Lin, S. H., "Statistical Behavior of a Fading Signal," B.S.T.J., *50*, No. 10 (December 1971), pp. 3311–3270.
4. Barnett, W. T., "Multipath Propagation at 4, 6, and 11 GHz," B.S.T.J., *51*, No. 2 (February 1972), pp. 321–361.